Letters

Boundary Conduction Mode Control of a Boost Converter With Active Switch Current-Mirroring Sensing

Mehrdad Biglarbegian, *Student Member, IEEE*, Namwon Kim, *Student Member, IEEE*, and Babak Parkhideh, *Senior Member, IEEE*

***Abstract*—This letter presents a control scheme to operate a boost converter in boundary conduction mode (BCM). In the proposed method, it is assumed that the zero-current information is not available for controlling the converter operation mode. Therefore, a cursor is identified to detect the converter operation mode, i.e., continuous conduction mode/BCM. Details of the cursor and associated control method will be discussed in this letter. We demonstrate experimentally the effectiveness of the proposed method on a GaN boost converter whose active switch current is monitored through a current-mirroring technique.**

***Index Terms*—Boundary conduction mode (BCM), current mirroring, dc–dc GaN boost converter, SenseFET, SenseGaN, zero current detection, zero current switching.**

I. Introduction

In (QUASI) soft-switching circuits, most attentions have been paid to zero-voltage switching due to the ease of voltage measurement and availability of passive components [1]. In power MOSFETs, turn-on losses are more dominant than turn-off losses [2]. Therefore, boundary conduction mode (BCM) operation is desirable in many power electronics converters [3]. To operate the converter at BCM, it is required to have a proper control scheme to change the switching frequency as well as an accurate method to detect the zero current.

Different zero current detection methods and associated control schemes for BCM operation have been proposed in recent literature. The current monitoring with isolated secondary winding of an inductor for unidirectional application is used in [4], dynamic current mirroring by memorization capability of charging capacitor is presented in [5], reverse current detection of inductor current by a freewheeling switch is implemented in [6], and online digital predictive BCM using equivalent series resistance of an inductor is provided in [7]. In a cost conscious yet efficient converters with voltage mode or duty cycle control, series-connected RC filters are used to detect the zero-current crossing point in [8] and [9]. For bidirectional converters, using a secondary winding only for zero current crossing detection has been proposed in [10]. Cost, bandwidth, and sensitivity at low currents are the reasons that isolated current sensors such as Hall-effect current sensors may not be the solution for many and emerging high-frequency power converters.

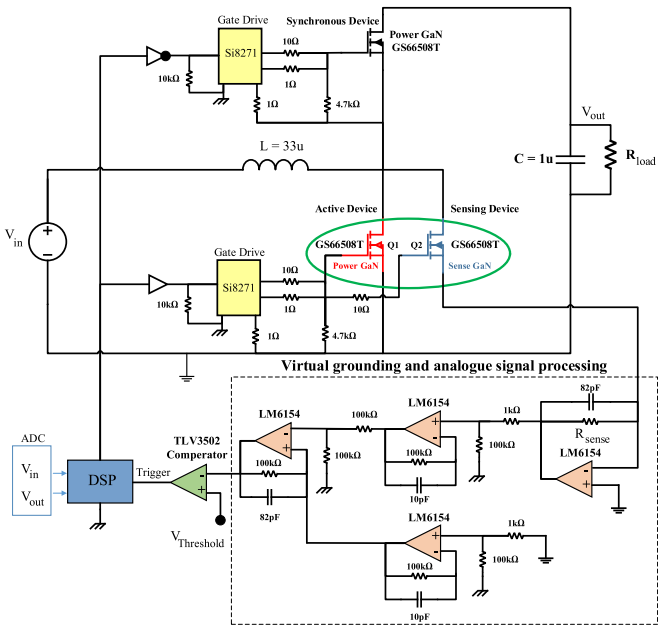

Fig. 1. Boost operation system with SenseGaN and control units.

The current mirroring technique can be used for monitoring the power device current practically in a loss-less manner compared to a shunt resistor method. In power electronics, current mirroring is commercialized and often known as the SenseFET approach. In this approach, two Si MOSFETs with different resistances are connected in parallel. The one with higher resistance carries much smaller current, yet can represent the current in the main branch with proportion. Recently, this approach has been demonstrated for SiC and GaN devices integrated with Si MOSFET in [11] and [12]. This approach can be cost effective if all integrated into the device die [13], [14]. However, the SenseFET is typically nonisolated, and hence, applicable for grounded devices where the common-mode voltage is higher than 30 V. For instance, the SenseFET in synchronous boost converters as

Manuscript received April 12, 2017; revised May 18, 2017; accepted June 10, 2017. Date of publication June 19, 2017; date of current version October 6, 2017. *(Corresponding author: Mehrdad Biglarbegian.)*

The authors are with Electrical and Computer Engineering Department, Energy Production and Infrastructure Center (EPIC), University of North Carolina-Charlotte, Charlotte, NC 28223 USA (e-mail: mbiglarb@uncc.edu; nkim22@uncc.edu; bparkhideh@uncc.edu).

Color versions of one or more of the figures in this letter are available online at http://ieeexplore.ieee.org.

Digital Object Identifier 10.1109/TPEL.2017.2716934

power factor correction circuit can be used in the active switch for controlling the converter in either continuous conduction mode (CCM) or discontinuous conduction mode (DCM).

In this letter, we propose a control scheme for a synchronous boost converter to operate in BCM. The active switch current is only sensed using the current mirroring technique. The challenge is the zero current for BCM operation obtained at the synchronous mode is not available for direct measurement. The converter operation mode cursor, i.e., CCM/BCM is identified through an adaptive comparison. The cursor is used in an iterative control scheme to bring the converter to BCM. The concept will be demonstrated on a boost converter using 650-V GaN devices. The current mirroring circuit has been implemented with the same GaN device for the active switch, which we call SenseGaN. The circuit details and experimental verification will be presented in Sections II and III, respectively. Section IV provides the conclusions.

II. Proposed BCM Control In a Boost Converter

A. Active Switch Current Measurement With SenseGaN

In this method, a parallel sensing GaN is used for the current mirroring of the active power module. The schematic of the sensing technique for a boost converter is shown in Fig. 1. Having the same gate signal source, and considering a virtual grounding to force the same drain–source voltage for both devices, then the voltage drop across the sensing resistor proportionally reflects the active transistor current. Therefore, a sensing GaN (Q2) can effectively monitor the current of Power GaN (Q1). Ideally, this technique is not limited by bandwidth, and can be perceived at the very high accurate measurement with significant low power loss. The compromise to choose the proper sensing resistor should be considered for the robustness of the system at higher switching frequency (smaller resistance) and lower loss (bigger resistance).

B. Proposed Algorithm for BCM Control

In the boost converter, since the SenseGaN can only be placed on the bottom side to avoid common-mode voltage issues, it can only measure the current during ON time. Assuming to run the converter with the same average current marked in Fig. 2(a), the measurement at CCM is more like perpendicular trapezoid; however, in BCM, the sensing element is characterized as a triangle shown in Fig. 2(b). This signature is used as an identifier to distinguish CCM and BCM. By monitoring of the input voltage and knowing the inductance value, the slope of the inductor current can be calculated in each cycle. Since the slope for both CCM and BCM are the same, an analogue delay trigger signal generated through a fast comparator is considered as a parametric identification value.

Due to the small input threshold voltage of the comparator, the SenseGaN device does not capture the diagonal linear region at CCM condition. Therefore, the generated trigger signal respect to the reference PWM has a zero delay; however, in BCM, the trigger signal compared to the reference PWM signal has a constant nonzero value. This delay can be calculated as: ($T_{\text{delay}} = L\frac{V_{\text{th}}}{V_{\text{in}}}$) where T_{delay} is the generated delay, V_{th} is the predefined input threshold voltage of the comparator, and V_{in}/L is the slope of the inductor current when the device is ON. The delay signal will be calculated in each cycle. Then, based on the captured delay, the control action can be updated sequentially to find the BCM of the converter.

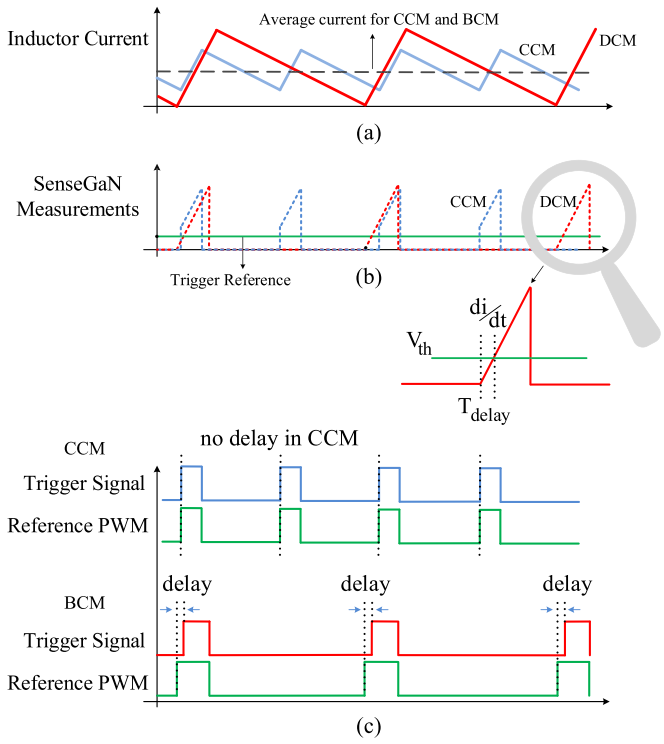

Fig. 2. System operation mode and curser identifications. (a) Inductor current at CCM (blue) and BCM (red) with the same average current. (b) Current monitoring with the SenseGaN for the active device in CCM and BCM. (Here, the zoomed-in version of threshold trigger reference signal for delay generation is exposed). (c) Microcontroller compares the trigger reference signal generated by the comparator and PWM signals to generate the delay signal in CCM and BCM.

The first part of the algorithm is to distinguish the CCM and BCM conditions. Here, once the load condition changes (for instance, higher current), the microcontroller captures a zero delay, thus, the converter operation is considered as CCM. Now based on the algorithm, the microcontroller gradually reduces the switching frequency to adaptively find the new BCM. This process will be continued till the generated nonzero delay matches with the calculated delay. Fig. 2(c) shows the delay comparisons of the algorithm in CCM and BCM.

The second part of the algorithm needs to be run to make sure the converter does not operate in DCM. This is very crucial because the generated delay signals in BCM and DCM have the same value. Here, by decreasing the switching frequency in small intervals from the BCM switching frequency, the controller can still observe the same delay signal, and the converter operation is perceived at DCM; On the other way, assuming to run the converter with calculated delay, by minor increasing the switching frequency once the BCM delay is detected, the converter operation will be entered to CCM. Therefore, the converter always operates in a narrow region as highlighted blue in Fig. 3.

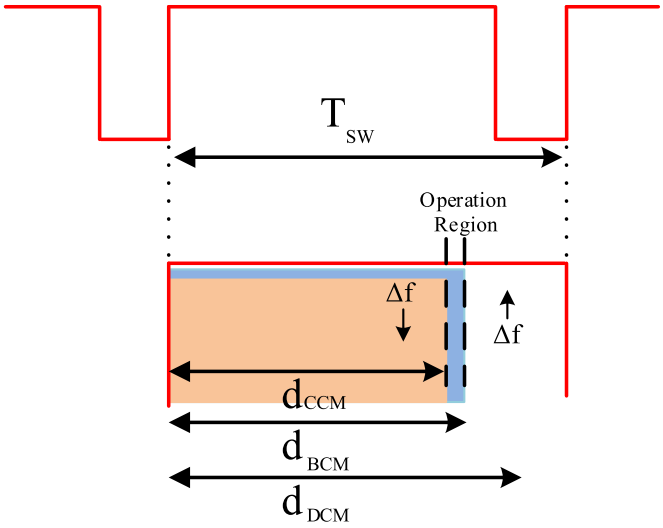

Fig. 3. Operational regions for distinguishing CCM, BCM, and DCM in a single cycle. Orange: CCM; Blue: Optimum region for BCM; Gray: DCM.

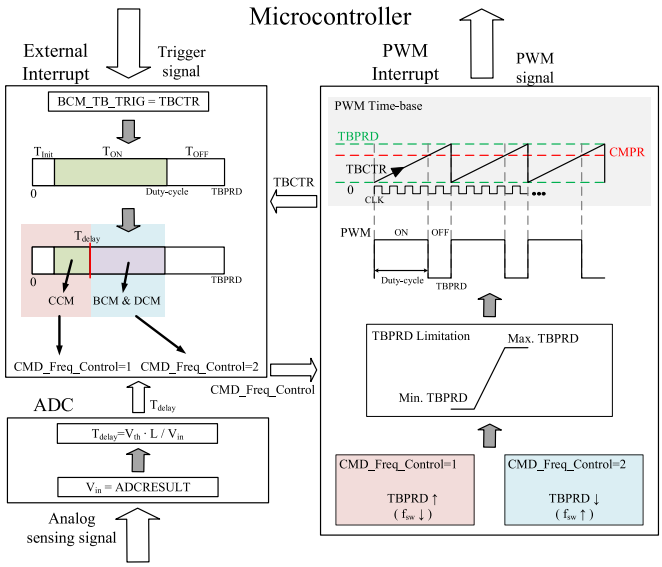

Fig. 4. Control scheme flow chart for the proposed BCM control algorithm.

Visualization of the details of the implemented BCM control of the boost converter in the microcontroller is shown in Fig. 4. The algorithm consists of interconnection of multiple functions as external interrupt (XINT), analogue to digital converter (ADC), and PWM Interrupt. For the microcontroller, two main inputs are required to create a criterion representing BCM conditions, and detection of the current state of the boost converter. The first one is the input voltage, and the other is the trigger signal. The analogue input voltage signal is applied to ADC for the delay time calculation, and the trigger signal enters to XINT for initiation of interrupt service routine.

Once the rising edge of the trigger signal is received, the microcontroller executes the XINT. Therefore, it calculates the elapsed time of the trigger signal with time-based counter register (TBCTR). The TBCTR is a counter register to generate PWM signal in a microcontroller. As shown in Fig. 4, initially

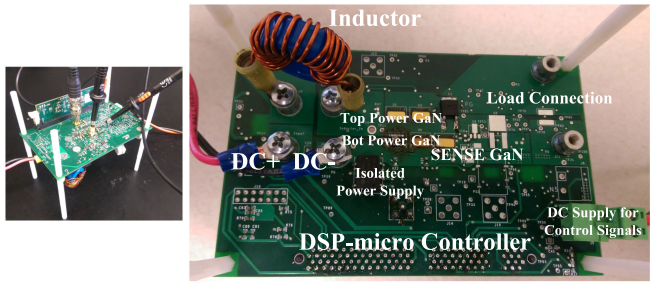

Fig. 5. *Hardware setup*: The prototype in four layers: TOP: Power stage; INNER-1: Power ground; INNER-2: Shielding; BOTTOM: Control signals.

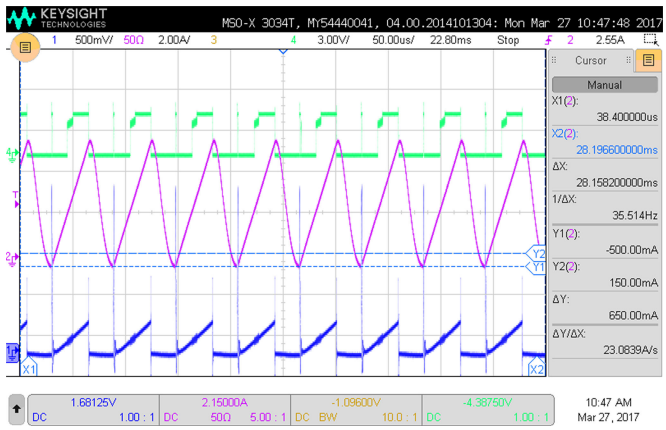

Fig. 6. *Experimental results*: SenseGaN operation at 2.5 A with 350-mV/A sensitivity. Purple: Inductor current measurement (amplifier current gun); Blue: SenseGaN measurement; Green: Generated trigger signal from the analogue comparator (TLV3502).

since TBCTR is zero, the PWM signal will be active high. When the TBCTR reaches to the counter compare register (CMPR), the high PWM signal is forced to low, and once TBCTR reaches the time-based period register (TBPRD), the TBCTR will be reset to zero. Since the TBCTR is synchronized with the PWM signal, the elapsed time of the trigger signal is calculated in each PWM cycle. Both CMPR and TBPRD are determined according to the operation condition of the boost converter.

Based on the calculation of the elapsed time, the status of the boost converter operation mode can be determined. If the trigger time is shorter than the delay time, it means that the boost converter is in CCM. If the trigger time is longer than the delay time, it means that the boost converter is in BCM/DCM. Since the slope of the inductor current will remain constant even at different operation conditions, the inductor current at CCM hits the threshold level faster than BCM/DCM.

Once the comparison is over, regulation of the PWM switching frequency is executed to keep the operation mode in BCM. If the operation mode is CCM, the TBPRD is increased to reduce the switching frequency. If the operation mode is the BCM/DCM, the TBPRD is decreased to raise the switching frequency. By updating the TBPRD, the operation mode is regulated. Since the trigger signal for both BCM/DCM is the same, repetitive increase of the switching frequency is required to guarantee the narrow region represented in Fig. 3.

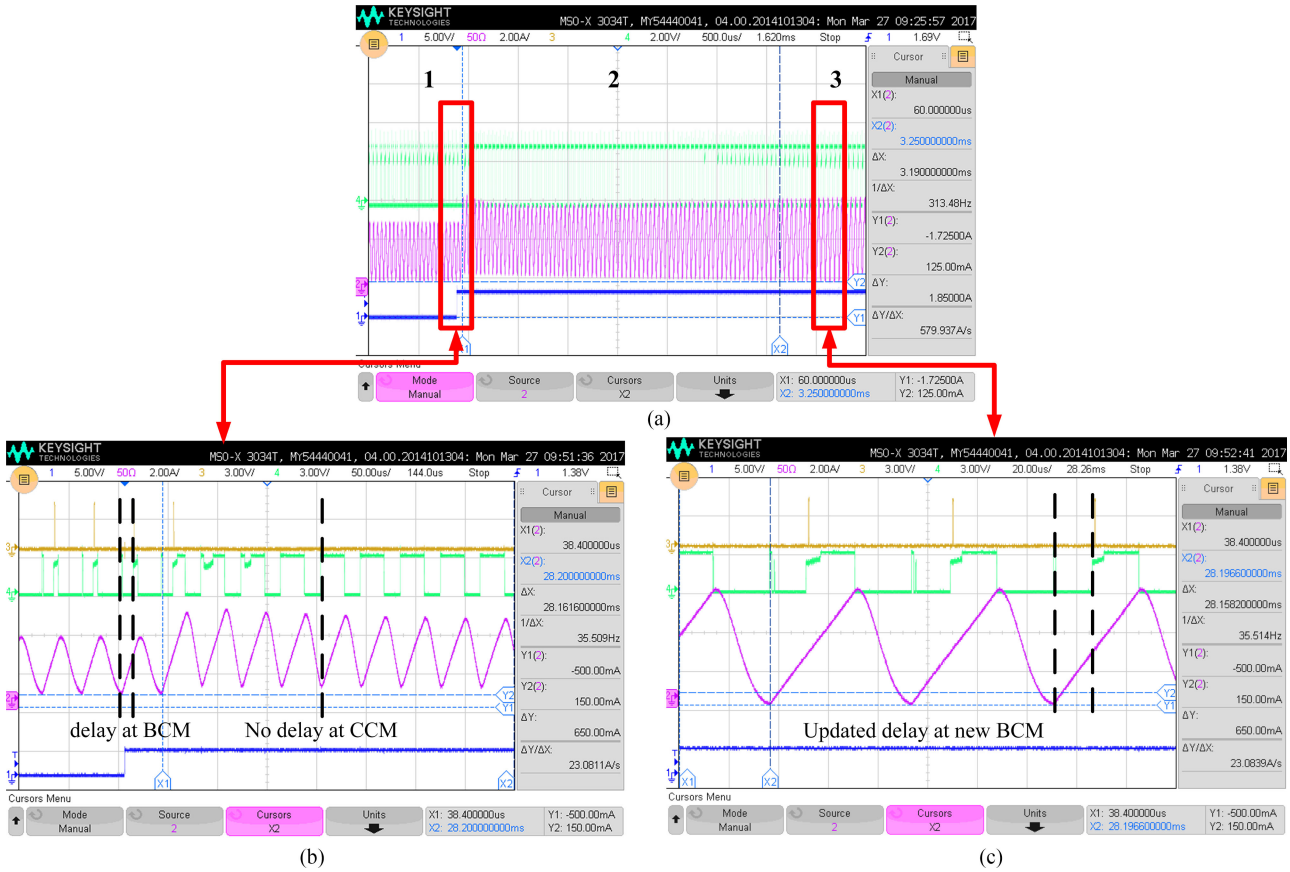

Fig. 7. *Experimental results*: Implementation of BCM in a boost converter with SenseGaN. Purple: Inductor current measured with an amplifier current gun; Green: Generated trigger signal with the fast comparator; Blue: Trigger signal for load change. (a) Converter operation at different CCM and BCM regions. (b) Initial BCM condition (duty cycle: 40%), and transient to CCM (60%). (c) New BCM steady-state condition for higher current after implementing the iterative control scheme. Delay detection between trigger signal and PWMs are highlighted in BCM and CCM operation.

III. Experimental Verification

To verify the effectiveness of the proposed method, a prototype was built in four-layer board presented in Fig. 5. On the top layers, all the power components including the GaN devices and inductors are placed. An additional shield is implemented in the inner layer to reduce the effect of switching noises on the measurements circuits. On the bottom layer, conditioning and controlling circuits including the microcontroller (TMS320F28335), ultrafast Op-Amps and comparators are placed. In this setup, 650-V/30-A GaN devices (GS66508T, $R_{\mathrm{ds(on)}} = 50\ \mathrm{m}\Omega$) and the isolated gate drivers (Si8271-GB-IS) were used. Furthermore, multiple design criteria were considered such as bigger resistor on the gate path of the SenseGaN (Q2). This is essential to have sufficient delays for proper current mirroring from the main power GaN (Q1) and avoid voltage transients. Since the input capacitance of the both Power and sensing devices are the same, a bigger precision resistor is also added to the gate path of the SenseGaN to bring a proper delay and avoiding high voltage transient. Ultrafast precision rail–rail Op-Amp (LM6154) with high common-mode rejection noise was used to provide virtual and firm ground. The sensing resistor is chosen as 20-Ω precision resistor with ultralow tolerance ($<0.1\%$). Multiple filter stages ($f_c < 1$ MHz) are also added to reduce the noise and achieve required signal scaling as shown in the schematic capture, Fig. 1. The converter was tested under different load conditions and switching frequencies to verify its sensitivity, linearity, and system robust operation. An example of the circuit operation with active switch current measurement using SenseGaN is represented in Fig. 6.

Initially, the converter operates at 40% duty cycle with 24 kHz under a resistive load of 8 Ω. As shown in Fig. 7, the converter operates in BCM and the delay is detected by the trigger signal. By increasing the duty cycle to 60%, the converter enters CCM and the trigger rising edge becomes equal to the active switch on time. In other words, there is no delay. This has been highlighted in Fig. 7(b). As mentioned, the delay makes sure the converter is in BCM. Through the microcontroller, the switching frequency sweeps with 1 kHz steps to reach the desirable delay, indicating the converter is practically in BCM. In this example, the BCM operation reaches 17 kHz and has been highlighted in Fig. 7(c).

IV. Conclusion

This letter presented a control scheme for the boost converter operating at BCM. The approach was through identifying a cursor that distinguishes between converter operation mode,

i.e., CCM/BCM. The cursor was generated incorporating the active switch current. The active switch current measurement was conducted by a current-mirroring technique applicable for grounded high-voltage power devices. It is believed that the current-mirroring technique can be integrated into emerging power semiconductor devices such as GaN. A representative circuit for such purpose was presented. The effectiveness of the proposed control scheme using the mode detection cursor was demonstrated experimentally.

REFERENCES

[1] K.-H. Liu and F. C. Lee, "Zero-voltage switching technique in DC/DC converters," *IEEE Trans. Power Electron.*, vol. 5, no. 3, pp. 293–304, Jul. 1990.

[2] S. Qin, Y. Lei, C. Barth, W.-C. Liu, and R. C. Pilawa-Podgurski, "A high power density series-stacked energy buffer for power pulsation decoupling in single-phase converters," *IEEE Trans. Power Electron.*, vol. 32, no. 6, pp. 4905–4924, Jun. 2017.

[3] T.-T. Song and H. S.-h. Chung, "Boundary control of boost converters using state-energy plane," *IEEE Trans. Power Electron.*, vol. 23, no. 2, pp. 551–563, Mar. 2008.

[4] H. Choi, "Interleaved boundary conduction mode (BCM) buck power factor correction (PFC) converter," *IEEE Trans. Power Electron.*, vol. 28, no. 6, pp. 2629–2634, Jun. 2013.

[5] V. Michal, "Inductor current zero-crossing detector and CCM/DCM boundary detector for integrated high-current switched-mode DC–DC converters," *IEEE Trans. Power Electron.*, vol. 29, no. 10, pp. 5384–5391, Oct. 2014.

[6] Y. Gao, S. Wang, H. Li, L. Chen, S. Fan, and L. Geng, "A novel zero-current-detector for DCM operation in synchronous converter," in *Proc. 2012 IEEE Int. Symp. Ind. Electron.*, 2012, pp. 99–104.

[7] Y.-T. Chang and Y.-S. Lai, "Online parameter tuning technique for predictive current-mode control operating in boundary conduction mode," *IEEE Trans. Ind. Electron.*, vol. 56, no. 8, pp. 3214–3221, Aug. 2009.

[8] S.-Y. Yu, "Design a transition-mode, bridgeless PFC with a standard PFC controller." Texas Instruments Inc., TX. 2014. [Online]. Available: http://www.ti.com/lit/an/slyt599/slyt599.pdf

[9] C. Bridge and L. Balogh, "Understanding interleaved boundary conduction mode PFC converters," Fairchild Semiconductor., CA. 2008. [Online]. Available: https://www.fairchildsemi.com/technical-articles/Understanding-Interleaved-Boundary-Conduction-Mode-PFC-Converters.pdf

[10] J. Biela, D. Hassler, J. Miniböck, and J. Kolar, "Optimal design of a 5 kW/dm3/98.3% efficient TCM resonant transition single-phase PFC rectifier," in *Proc. IEEE Int. Power Electron. Conf.*, 2010, pp. 1709–1716.

[11] P. Liu, L. Zhang, A. Q. Huang, S. Guo, and Y. Lei, "High bandwidth current sensing of SiC MOSFET with a Si current mirror," in *Proc. 2016 IEEE 4th Workshop Wide BandGap Power Devices Appl.*, 2016, pp. 200–203.

[12] Y. Wen, M. Rose, R. Fernandes, R. Van Otten, H. J. Bergveld, and O. Trescases, "A dual-mode driver IC with monolithic negative drive-voltage capability and digital current-mode controller for depletion-mode GaN HEMT," *IEEE Trans. Power Electron.*, vol. 32, no. 1, pp. 423–432, Jan. 2017.

[13] ON Semiconductor, *AND8093/D, Current Sensing Power MOSFETs*, Semiconductor Components Industries, LLC, Phoenix, AZ, USA, pp. 1–12, 2002.

[14] A. Furukawa *et al.*, "Low on-resistance 1.2 kV 4H-SiC MOSFETs integrated with current sensor," in *Proc. 2011 IEEE 23rd Int. Symp. Power Semicond. Devices ICs*, 2011, pp. 288–291.